Electronic structure of hybrid interfaces for polymer-based electronics

2007 J. Phys.: Condens. Matter 19 183202

(http://iopscience.iop.org/0953-8984/19/18/183202)

IOP PUBLISHING JOURNAL OF PHYSICS: CONDENSED MATTER

J. Phys.: Condens. Matter **19** (2007) 183202 (20pp) doi:10.1088/0953-8984/19/18/183202

TOPICAL REVIEW

Electronic structure of hybrid interfaces for polymer-based electronics

M Fahlman[1], A Crispin[2], X Crispin[1], S K M Henze[1,3], M P de Jong[2], W Osikowicz[2], C Tengstedt[1] and W R Salaneck[2]

[1] Department of Science and Technology, Linköping University, 60174 Norrköping, Sweden
[2] Department of Physics, Chemistry and Biology, Linköping University, 58183 Linköping, Sweden

Received 15 August 2006, in final form 2 February 2007
Published 4 April 2007
Online at stacks.iop.org/JPhysCM/19/183202

Abstract

The fundamentals of the energy level alignment at anode and cathode electrodes in organic electronics are described. We focus on two different models that treat weakly interacting organic/metal (and organic/organic) interfaces: the induced density of interfacial states model and the so-called integer charge transfer model. The two models are compared and evaluated, mainly using photoelectron spectroscopy data of the energy level alignment of conjugated polymers and molecules at various organic/metal and organic/organic interfaces. We show that two different alignment regimes are generally observed: (i) vacuum level alignment, which corresponds to the lack of vacuum level offsets (Schottky–Mott limit) and hence the lack of charge transfer across the interface, and (ii) Fermi level pinning where the resulting work function of an organic/metal and organic/organic bilayer is independent of the substrate work function and an interface dipole is formed due to charge transfer across the interface. We argue that the experimental results are best described by the integer charge transfer model which predicts the vacuum level alignment when the substrate work function is above the positive charge transfer level and below the negative charge transfer level of the conjugated material. The model further predicts Fermi level pinning to the positive (negative) charge transfer level when the substrate work function is below (above) the positive (negative) charge transfer level. The nature of the integer charge transfer levels depend on the materials system: for conjugated large molecules and polymers, the integer charge transfer states are polarons or bipolarons; for small molecules' highest occupied and lowest unoccupied molecular orbitals and for crystalline systems, the relevant levels are the valence and conduction band edges. Finally, limits and further improvements to the integer charge transfer model are discussed as well as the impact on device design.

(Some figures in this article are in colour only in the electronic version)

[3] Present address: School of Engineering and Science, International University Bremen, PO Box 750561, 28725 Bremen, Germany.

0953-8984/07/183202+20$30.00

Contents

1. Introduction 2
2. Experimental details 4
3. Results 6
4. Summary and discussion 18
References 19

1. Introduction

Organic-based electronics [1] such as plastic memory, light emitting displays [2], transistors [3] and plastic solar cells [4, 5] are under development, and applications (displays) have already reached the market. Research on molecular-scale electronics [6] based on (organic) molecular wires [7, 8] also show some promise, but are unlikely to produce applications in the near future. Of particular interest in the field of organic electronics are so-called bulk heterojunction solar cells and organic-based light emitting diodes for lighting applications, since they are positioned to have a huge impact on how we obtain energy and use it more efficiently. One of the key issues for both those technologies is the understanding of the energy level alignment at organic/organic and organic/metal interfaces. Proper matching of the electrode Fermi levels to the charge carrying species (polarons) in the electroluminescent polymers (ELP) is necessary to obtain efficient charge injection in, for example, organic and polymer light emitting devices (OLEDs and PLEDs). The energetics of organic/organic hetero-interfaces in organic-based solar cells is of crucial importance for efficient charge separation and significantly affects the open-circuit voltage as well. However, no consensus exists on how to model such interfaces properly, much to the detriment of device development. A vast number of competing theories have been proposed, but currently two main models for weakly interacting organic/metal and organic/organic interfaces are under study, and the main concepts (without the finer details) of the two models are outlined below.

The so-called 'induced density of interfacial states' (IDIS) model proposes that charge transfer occurs over organic/metal interfaces so that the Fermi level of the metal aligns with the so-called charge neutrality level (CNL) of the organic molecule modified by a screening parameter S [9, 10]. The key idea of this model is that the resonance of molecular states with the metal continuum of states gives rise to a shift and broadening of the molecular levels, and that each molecular level is broadened into a Lorentzian function (still assuming weakly interacting interfaces and not chemisorption). The sum of the contributions of the different molecular levels transforms the initial 'discrete' distribution into a continuum density of states (DOS) with non-negligible values in the former energy gap. By filling this induced DOS by the charge of the isolated and neutral molecule/polymer, the position of the CNL is obtained. The relative position of the semiconductor CNL and substrate Fermi level determines the direction and size of the charge transfer. (Convention dictates that the Fermi level is typically set at zero binding energy and the value of the work function (Φ_{SUB}) is used instead.) The initial CNL $-$ Φs difference is reduced by the S parameter so that the interface Fermi level position (E_{F}) and induced dipole (Δ) are given by [9, 10]:

$$E_{\mathrm{F}} - \mathrm{CNL} = S(\Phi_{\mathrm{SUB}} - \mathrm{CNL}) \tag{1}$$

$$\Delta = (1 - S)(\Phi_{\mathrm{SUB}} - \mathrm{CNL}) \tag{2}$$

$$S = \mathrm{d}E_{\mathrm{F}}/\mathrm{d}\Phi_{\mathrm{SUB}} = 1/(1 + 4\pi e^2 D(E_{\mathrm{F}})\delta/A) \tag{3}$$

where $D(E_{\mathrm{F}})$ is the DOS of the interface molecules at E_{F} (given the modifications discussed above, i.e. a continuum DOS), δ is the distance between the molecule and the substrate, and A

is the interface area of the molecule. The same model is proposed for organic/organic interfaces as well, in which case the two charge neutrality levels align, modified by the S-parameter [10]. Hence, if this model is correct, weakly interacting organic/organic and organic/metal interfaces should also yield a linear dependence between the interface Fermi level position and the substrate work function, with a slope ranging between 0 and 1.

The other model is, at first glance, fairly similar, but produces a completely different behaviour for the E_F versus Φ_{SUB} dependence. The so-called integer charge transfer (ICT) model [11–14] also predicts that new states may be induced in the organic molecules/polymers at weakly interacting interfaces, but the mechanism for the induced states and their nature are different, namely, if spontaneous charge transfer occurs across the interface via tunnelling processes, then discrete charge transfer states are created, not a (quasi) continuum of states as in the IDIS model. The difference thus lies in the degree of mixing between the π-electronic wavefunctions of the adsorbed molecules or polymers with the substrate wavefunctions (continuum states for metals): if this mixing is significant then the IDIS approach is valid, whereas if it is negligible then the ICT model applies. Furthermore, the ICT model predicts integer charge transfer, whereas the IDIS model predicts partial electron exchange. In the particular case of conjugated large molecules and polymers, the integer charge transfer states that are created are polaronic in nature. Conjugated polymers are 'soft' materials, so any reduction or addition of charge to such a system creates a *geometric* relaxation as well as an electronic relaxation, which leads to self-localized states that are called polarons (single charge) or bipolarons (double charge). This creates states separated from the HOMO/LUMO (highest occupied molecular orbital/lowest unoccupied molecular orbital) edges of the neutral molecule/polymer, and the polarons/bipolarons then appear as new features in the previously forbidden band gap; see figure 1. Note that polarons and bipolarons are intrinsic charge carrying states of conjugated systems (with non-degenerate ground states) and are induced at the interface by charge transfer to/from the substrate when energetically favourable. Hence, for large conjugated molecules and polymers the ICT model predicts so-called vacuum level alignment [15] (Schottky–Mott limit) when Φ_{SUB} is greater than the formation energy of a negative polaron/bipolaron (E_{P-}/E_{BP--}) and smaller than the formation energy of a positive polaron/bipolaron (E_{P+}/E_{BP++}). (The formation energy of a positive polaron is here defined as the energy required to take away one electron from the molecule/polymer, producing a fully relaxed state, i.e. both electronic and geometrical relaxation is included.) The ICT model further predicts that Fermi level pinning to the positive polaron/bipolaron level of the molecule/polymer occurs when Φ_{SUB} is greater than E_{P+}/E_{BP++}, and that Fermi level pinning to the negative polaron/bipolaron level of the molecule/polymer occurs when Φ_{SUB} is smaller than E_{P-}/E_{BP-} [14]. Hence, if the substrate work function is swept through a range of small to large values that is large enough to fulfill $\Phi_{SUB} < E_{P-}/E_{BP--}$, $E_{P-}/E_{BP--} < \Phi_{SUB} < E_{P+}/E_{BP++}$ and $\Phi_{SUB} > E_{P+}/E_{BP++}$, the integer charge transfer model would predict a 'Mark of Zorro' dependence of E_F versus Φ_{SUB} (figure 2(a)), whereas the IDIS model predicts a linear function with a slope S between 0 and 1 (figure 2(b)), as mentioned above. The two models are thus, despite many similarities, mutually exclusive. Note that the integer charge transfer model obviously also applies to systems lacking polaronic states, such as small conjugated organic molecules or crystalline molecular films with band-like electronic structure. Here the positive charge transfer state (E_{ICT+}) corresponds to the highest occupied molecular orbital (or valence band edge) and the negative charge transfer (E_{ICT-}) state corresponds to the lowest unoccupied orbital (or conduction band edge). The three generalized equations are then: $\Phi_{SUB} < E_{ICT-}$, $E_{ICT-} < \Phi_{SUB} < E_{ICT+}$ and $\Phi_{SUB} > E_{ICT+}$ for positive charge transfer pinning, vacuum level alignment and negative charge transfer pinning, respectively.

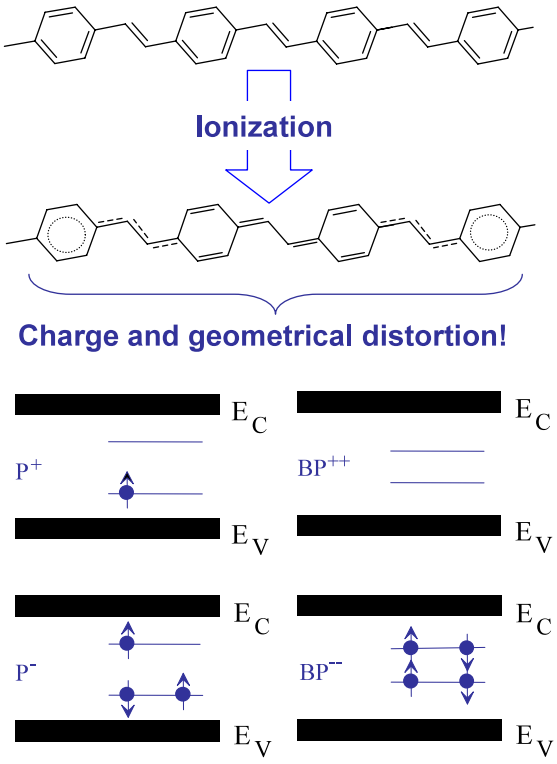

Figure 1. Schematic picture of polaron and bipolaron states (geometry and energy) in conjugated organic systems.

As noted earlier, proper energy level matching at metal/organic and organic/organic heterojunctions is crucial for device design and performance, and it is thus to great detriment that a consensus for how to describe and model the energetics at such interfaces properly does not exist today. Until such a model is established, device design will continue to be a trial-and-error process and proper modelling of device operation cannot be done without the correct understanding and knowledge of the interface energetics that is lacking today. In this paper we will argue in favour of the integer charge transfer model for the description of various interfaces encountered in organic electronic applications and present results in support thereof. We believe that this model offers the basis for a comprehensive and accurate description of weakly interacting organic/metal and organic/organic interfaces in organic electronics.

2. Experimental details

The data discussed in this review paper is derived mainly from photoelectron spectroscopy (PES) [16, 17]. PES is a widely used tool for studying the bulk and surface chemical and electronic structure of condensed matter. In particular, the method is very useful for studies of the chemical and electronic structure of surfaces and interfaces, as it provides a maximum amount of chemical and electronic information within a single technique, is essentially non-destructive to most material systems, and the method is extremely surface sensitive. While the path length in the samples of the photons typically used in photoelectron spectroscopy is of the order of micrometres, the electron inelastic mean free path λ is typically on the order of tens of ångströms for x-ray photoelectron spectroscopy (XPS) [16] and less than 10 Å for ultraviolet photoelectron spectroscopy (UPS) [17]. Hence, while ionization occurs all the way down to

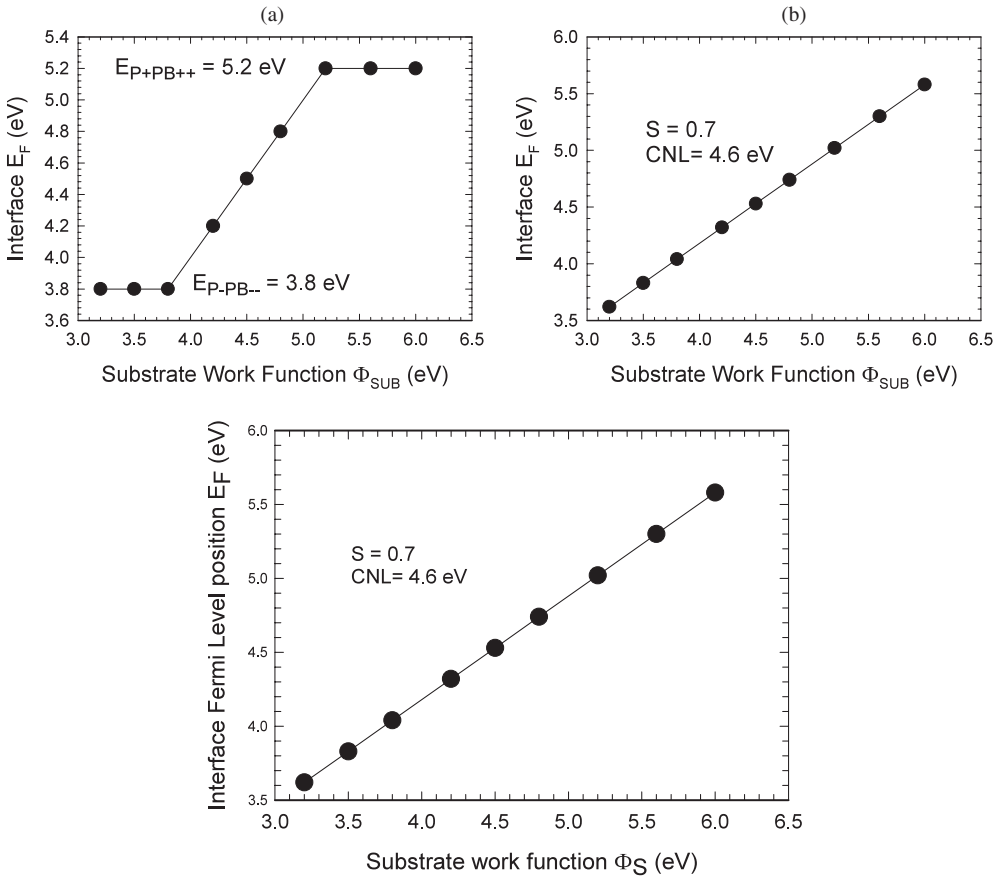

Figure 2. Hypothetical polaronic-pinning E_F versus Φ_{SUB} dependence ((a), left panel). Hypothetical IDIS E_F versus Φ_{SUB} dependence ((b), right panel).

micrometre depths for both x-rays and ultraviolet light, the electrons that originate within 3λ below the sample surface make up 95% of the signal [18].

The basic equation used in interpreting photoelectron spectra can be written as

$$E_B^v = E_+^* - E_0 = h\nu - E_k. \tag{4}$$

The photon energy $h\nu$ is known and the photoelectron kinetic energy distribution is measured in order to deduce the binding energy referenced to the vacuum level, E_B^v. The binding energy is thus not equal to the binding energy of the electrons in the neutral ground state, E_0, but corresponds to the energy difference between the initial ground state and various final excited states, E_+^*. During the photoelectron emission event there are electronic relaxation effects occurring. These effects can be rationalized, in a *classical picture*, as follows: an electron in a photoelectron emission event leaves a molecule typically within about 10^{-15} s. The nuclear geometric relaxation time is around 10^{-13} s (i.e., which corresponds to an optical phonon frequency) while the corresponding electronic relaxation time is about 10^{-16} s [19]. Thus, the electrons have had time to relax, i.e. the hole is fully screened, but the nuclei are frozen during the process. This means that for systems where the ionized final state energy is significantly affected (lowered) by geometric relaxation, which is the case for most π-conjugated organic molecules, PES measurements may overestimate the binding energy.

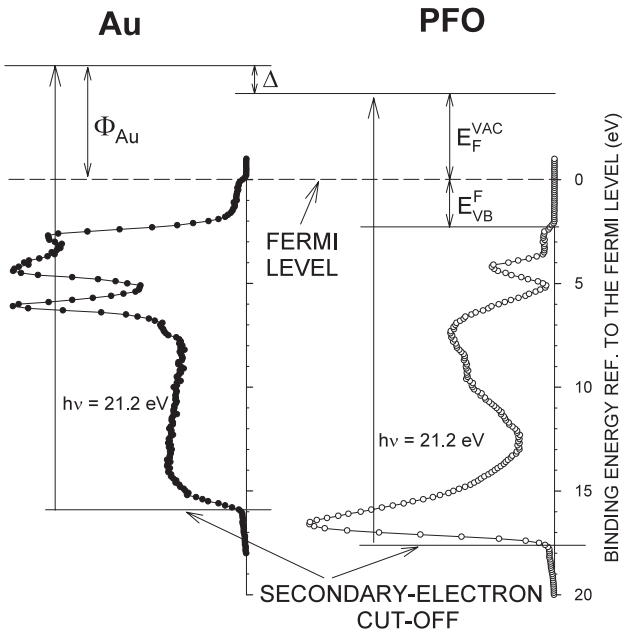

Figure 3. Schematic illustration of important parameters derived from UPS characterization of the interfaces.

XPS enables the study of qualitative and even semi-quantitative analysis of chemical composition in the near surface region of a solid sample. Changes in the valence electron density will be reflected as small but significant shifts in the core level binding energies, so-called chemical shifts, even though the core electrons are not involved in the chemical bonds [16]. Hence, charge transfer and chemical bond formation can be probed using XPS. The valence electronic structure is typically studied using UPS, however, as UPS has two advantages over XPS in such experiments. First, the photoionization cross section for electrons is orders of magnitude higher in the valence region for UPS and, second, the usual in-house photon sources (He resonance lamps) have high energy resolution, a full width at half maximum (FWHM) of ∼30 meV for the He lines.

3. Results

The ICT model predicts vacuum level alignment at weakly interacting organic/metal interfaces when Φ_{SUB} is greater than the formation energy of a negative integer charge transfer state ($E_{ICT-} = E_{P-}/E_{BP--}$ for conjugated polymers) and smaller than the formation energy of a positive integer charge transfer state ($E_{ICT+} = E_{P+}/E_{BP++}$ for conjugated polymers), which in either case would prevent charge transfer across the interface. We illustrate the vacuum level alignment regime of polymer-on-metal interfaces by a combined UPS and XPS study of energy level alignment of the electroluminescent polymer poly(9,9-dioctylfluorene), PFO, spin-coated under ambient (air) conditions onto a variety of substrates [15]. The issue of band bending in pristine polymer films was also addressed in this study, as films of PFO with thicknesses of 50 to 1100 Å were studied [15]. The energy level parameters have been obtained from the UPS data, as sketched in figure 3, where experimental spectra for a gold substrate (black dots) and a PFO polymer film (white dots) are depicted. The key parameters obtained from the UPS measurement are the following:

(i) E_F^{VAC}, the energy difference between the vacuum level of the organic film and the Fermi level of the (conducting) substrate;

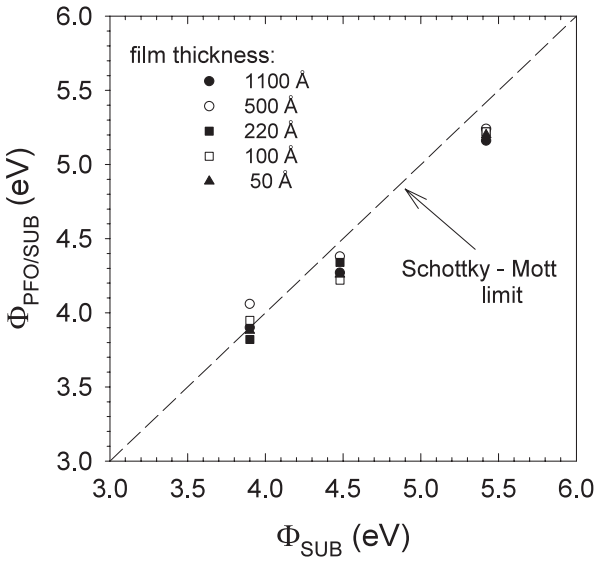

Figure 4. UPS measured dependence of the work function of PFO-coated substrates, $\Phi_{PFO/SUB}$, on the work function of the bare substrate for PFO films of different thickness: 50, 100, 220, 500 and 1100 Å.

(ii) E_{VB}^{F}, the difference in kinetic energy between the fastest electrons escaping from the conducting substrate and from the organic film itself which, in turn, corresponds to the offset between the Fermi level of the substrate and the valence band (VB) edge (highest occupied molecular orbital, HOMO, for molecules) in the polymer (molecule) UPS spectrum;

(iii) Δ, the energy offset between the vacuum level of the substrate and the vacuum level of the organic film;

(iv) Φ_{Au}, the work function of the substrate (in this example gold), as determined from the position of the cutoff of the secondary electrons, where $\Phi_{Au} = h\nu - E_{(cut-offforAu)}$.

Two related issues should be emphasized. First, the sum of E_{F}^{VAC} and E_{VB}^{F} is equal to the ionization potential (IP) of the polymer and constitutes a specific property of the material, independent of the energy level alignment at the interface. Second, note also that the IP measured by UPS does not include the geometric relaxation energy, which can be quite large for conjugated polymers and molecules.

Figure 4 [15] shows the main results from the study: changes in E_{F}^{VAC} for the PFO films as a function of the work function of the substrate. The work functions of the substrates (Al_xO_y, SiO_2 and ozone-treated Au) were found to be 3.9, 4.4 and 5.4 eV, respectively. PFO films of different thicknesses varying from 50 to 1100 Å were studied on each of the three different substrates. In each case, the position of the vacuum level of PFO as measured from the Fermi level, E_{F}^{VAC}, approximately followed the Schottky–Mott limit (long-dashed line), As the Fermi energy changes from 3.9 eV for aluminium oxide to 5.4 eV for ozone-treated gold, E_{F}^{VAC} increases from 3.9 to 5.2 eV, which implies alignment of the vacuum levels at the interface between PFO and the conducting substrates, though small deviations were seen for the case of ozone-treated gold substrate. As PFO has a large IP of 5.8 eV, these results were not surprising, since charge transfer from the valence band edge of the PFO into the substrates across the interface would seem to be energetically unfavourable, given the work function of the substrates involved. Without charge transfer across the interface, no potential drop at the

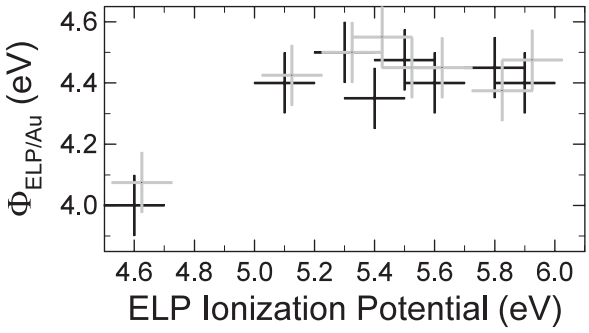

Figure 5. Summarized results of the UPS measured work function of a series of interfaces: vapour-deposited gold on polymer, Au/polymer (filled markers) and spin-coated polymer on gold, and polymer/Au (empty markers). For the sake of clarity, the polymer/Au points are artificially shifted 0.025 eV on the IP scale.

interface is expected and the vacuum level alignment regime is obtained. As a consequence, the entire UPS spectrum experiences a rigid shift in binding energy, up to 1.3 eV, when the work function of the substrate is varied. Note that E_{VB}^{F} changes by the same amount as E_{F}^{VAC}, since they are related through the IP of the organic material. This behaviour is very important for polymer light emitting devices, since such significant shifts cause large changes in the barrier heights for carrier injection at the interfaces between the polymer and the electrode contacts. The results above indicate also that for PFO films the energetics at weakly interacting polymer/metal interfaces is *independent of the film thickness*. This means that the flat band regime extends at least to 1100 Å from the interface!

The vacuum level alignment regime is also demonstrated in a separate study of weakly interacting interfaces of electroluminescent polymers (ELPs) spin-coated on polycrystalline gold and gold vacuum deposited on spin-coated ELPs [20]. The gold substrates were cleaned in acetone and isopropanol prior to spin-coating with ELPs. However, after such treatment, the gold surfaces were not atomically clean and produced a work function of 4.5 ± 0.1 eV. In the second case, several hundreds of nanometres thick Au films were deposited in UHV (ultrahigh vacuum) onto ELP films (spin-coated onto weakly adherent substrates such as Teflon and silicon oxide), whereupon the two-layered Au/ELP structures were peeled off using adhesive tape and inverted on the sample holder so that the *polymer side* of the bilayer structure could be studied by UPS. (The peeling off and sample inversion was performed in ambient conditions.) The ELPs were chosen so that their IPs spanned from 4.6 to 5.9 eV. The results from UPS measurements are summarized in figure 5 [20], where the resulting work functions of the ELP-on-Au and Au-on-ELP bilayer structures are displayed. For all ELP studied with IPs substantially higher than the 'dirty' gold work function of 4.5 eV, the measured work function of the bilayer structure was 4.4–4.5 eV, suggesting vacuum level alignment between the ELPs and the gold film. This behaviour is readily explained by the polaron-pinning model, as spontaneous charge transfer from the ELP valence band edge to the gold film at the interface is unlikely, given the large offset between ELP IP and the 'dirty' gold work function.

A possible way to model the experimental results using the IDIS approach would be to set $S = 1$ in all cases, which could be justified by stating that charge transfer between the ELP and the gold is hindered by the couple of monolayers (approximately) of hydrocarbon contamination on the gold surface for the case of ELPs spin-coated on gold [21–23]. Note that this is a necessary assumption since, given the large variation in IPs, the CNLs should vary as well and hence produce a range of interface offsets, $\Delta = (1 - S)\ (\Phi_{SUB} - \mathrm{CNL})$,

which is not the case. On a similar note, a variation in the screening factor S is also unlikely, given that the substrate is the same and all samples are prepared by spin-coating in ambient conditions, producing weakly interacting physisorbed films. Therefore, the model may hold only if the contaminating (mono)layers are assumed to decouple the organic film from the continuum of the metallic electronic states, which also in turn reduces the DOS induced in the gap of the organic material, yielding screening factors S close to or equal to 1, as demonstrated in a recent study [22]. The same conditions hold true for the results presented in figure 4, as all ELP films were spin-coated in ambient conditions and the substrates would then be expected to have at least a monolayer (approximately) of hydrocarbon contamination, despite chemical (and ozone) cleaning treatments. Similarly, the thin insulating surface layer found in many poly(3,4-ethylenedioxythiophene)—(PEDOT) and polyaniline-based conductive polymer blends [24–26] would also then be expected to prevent charge transfer across the interface, yielding an $S = 1$ and hence vacuum level alignment, as suggested in a recent paper [21].

In the 'dirty' gold study presented in figure 5 [20], it is interesting to note that the Au-on-ELP samples give identical results to those of ELP-on-Au, yet in the former case no hydrocarbon contaminant is present, as the Au was deposited onto the ELP films in UHV. Furthermore, no chemical modification of the films occurred, so chemical modification at the interface cannot be invoked to explain this result. Instead it was proposed that the comparatively low work function obtained was due to the well-known 'push-back' effect, i.e. the surface dipole of the gold layer is decreased due to the compression of the electron density tail in the presence of an organic contact layer [27–30]. Hence, whether it is hydrocarbon contaminants or ELPs physisorbed on a gold surface, the resulting work function of the metal substrate is expected to be decreased. This 'push-back' effect can thus be of huge importance, as illustrated by the above results, and we hence will discuss the concepts involved in greater detail.

The evolution of the electrostatic potential $\phi(x)$ across the metal/vacuum interface is related to the difference between the electron density $\rho(x)$ and the nucleus density. In the jellium model, the nucleus density is represented by a step function, i.e. it drops to zero at the metal surface (the jellium edge); on the other hand, the electron density of a metal surface decreases exponentially over several ångströms away from the surface plane of the metal nuclei [31]. A neutral metal surface in vacuum presents a surface dipole, since there is a deficit of electronic density $\rho(x)$ (bottom dotted curve, figure 6) inside the metal close to the surface, while an excess of electronic density is obtained outside the surface (electrons tunnel into the vacuum). As a consequence, the electrostatic potential $\phi(x)$ (top full line, figure 6) jumps from its bulk value ϕ^{in} (inner potential) to a higher value ϕ^{out} outside the metal (outer potential). If the zero energy is set at E_{F}, $\phi(x)$ tends exponentially to the work function. The difference between the inner and outer electrostatic potentials defines the metal surface dipole potential energy, $eD_{\text{met}} = e(\phi^{\text{out}} - \phi^{\text{in}})$, which can reach several eV. For a metal surface represented by the jellium model described in the framework of the density functional theory (DFT), the work function is composed of a bulk parameter $\bar{\mu}^{\text{DFT}}$, the DFT internal chemical potential, and a surface parameter D_{met} (equation (5)) [32]. The surface dipole potential energy has been evaluated by Lang as the difference between the calculated DFT bulk chemical potential $\bar{\mu}^{\text{DFT}}$ and the experimental work function Φ. For nickel, D_{met} is estimated to be about 4.2 eV:

$$\Phi = -\bar{\mu}^{\text{DFT}} + eD_{\text{met}}. \tag{5}$$

It has been shown theoretically that the presence of a physisorbed species leads to a shortening of the electron density tail at the metal surface. As a result, the metal surface dipole potential D_{met} is expected to be significantly reduced and the work function decreased by the same amount (see equation (5)) [29]. The metal surface dipole change upon physisorption

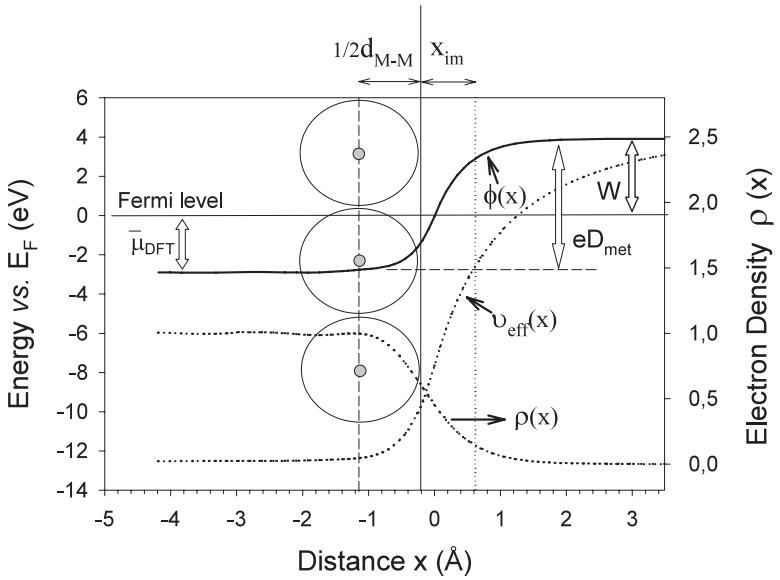

Figure 6. DFT calculations within the jellium model by Lang and Kohn give the evolution of the electron density $\rho(x)$ across the metal/vacuum interface (bottom dotted curve), the effective potential $\upsilon_{\text{eff}}(x)$ (top dotted curve), and the electrostatic potential $\phi(x)$ (top solid line). The large circles depict the atoms on the metal surface; the zero on the x axis is positioned at half the interatomic layer distance ($\frac{1}{2}d_{\text{M-M}}$) from the surface nuclei plane ($x > 0$ indicates the metal bulk); x_{im} defines the image plane position.

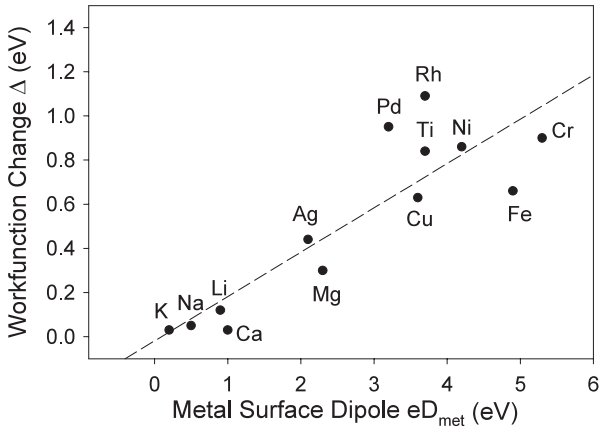

Figure 7. Evolution of the work function change of various metals upon adsorption of a Xe monolayer, with respect to the metal surface dipole.

can be illustrated with the archetype system for physisorption: Xe adsorbed on various metal surfaces. Figure 7 confirms that the work function changes, for one Xe monolayer coverage (as reported by Chen *et al* [33]), are related to the metal surface dipole estimated by Lang *et al* from jellium model calculations. To a first approximation, a linear relation $\Delta \cong 0.2 \times eD_{\text{met}}$ can be extracted from figure 7 [33] and considered as a characteristic feature for physisorption. The larger the metal surface dipole, the more polarizable the electron density tail at the surface and the larger the change in work function upon physisorption.

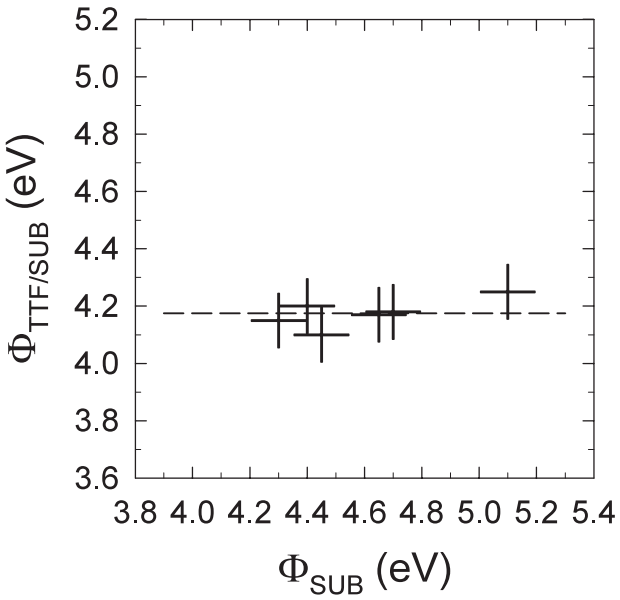

Figure 8. Dependence of work function of TTF *in situ* coated substrate, $\Phi_{TTF/SUB}$, on the work function of the bare substrate, Φ_{SUB}, as measured by UPS.

The decrease in work function obtained for the weakly interacting polymer-on-gold interfaces compared to clean gold can thus be reconciled with vacuum level alignment by taking into account the push-back effect. However, the deviation of the regio-regular P3HT points in figure 5 [20], ∼0.4 eV lower work function compared to the other ELPs, deserves further scrutiny, as does perhaps the PFO on ozone-treated gold points in figure 4 [15], as they are ∼0.2 eV lower than the expected value for vacuum level alignment. In the latter case, push-back could be invoked as an explanation, since the decrease is quite small. However, on the other hand, the ozone-treated gold substrate has a pacified surface already prior to ELP spin-coating and is hence not expected to show any further modification due to shortening of the metal electron density tail. For the P3HT data, another explanation clearly must be sought, as the overall modification of −1.1 eV compared to bare polycrystaline gold is unrealistically large for it to be caused by the push-back effect alone. Also, since the 'dirty' gold surface is already pacified prior to spin-coating for the P3HT-on-Au samples (as for other polymer-on-Au samples), an extra downshift of 0.4 eV could hardly be expected. Such deviations from the vacuum level alignment regime have in fact been seen in studies on weakly interacting conducting polymer-on-metal interfaces as well [34]. There the interpretation was that Fermi level alignment occurred at equilibrium due to charge transfer across the interface between the two metallic systems [34]. Conducting polymers, having a well-defined Fermi level, thus act as normal metals in terms of energy level alignment at interfaces, i.e. the resulting work function of a bilayer structure is *independent* of the substrate work function [34]. Substrate-independent behaviour of the work function of organic-on-metal interfaces in fact has been demonstrated for many systems of pristine conjugated molecules as well, including tetrathiafulvane, TTF; see figure 8 [35]. In that study, TTF molecules were deposited under UHV *in situ* conditions onto pacified metallic surfaces such as acetone- and isopropanol-washed (ozone-treated) gold, acetone- and isopropanol-washed indium tin oxide (ITO) and PEDOT-PSS. Regardless of the substrate work function, the TTF overlayer produced a work function of 4.2 eV. No evidence of chemical modification the TTF molecules were present in the XPS and UPS spectra, and the modification of the substrate work functions were attributed to charge transfer from the HOMO

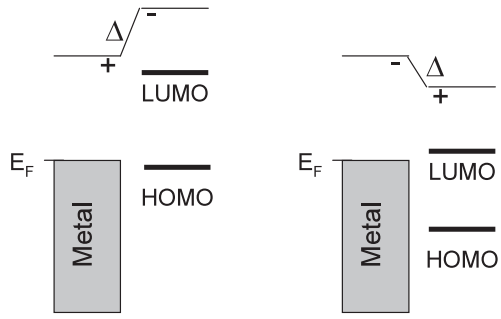

Figure 9. Schematic picture of a charge-transfer-induced interface dipole that upshifts the work function (electrons transferred *from* the substrate, left) and of a charge-transfer-induced interface dipole that downshifts the work function (electrons transferred *to* the substrate, right).

level of the TTF molecules at the interface into the DOS close to the substrate Fermi level [35]. Charge transfer across the interface will result in the formation of an interfacial dipole that downshifts the work function when electronic charge is transferred to the substrate and upshifts the work function when charge is transferred from the substrate [36, 37]; see figure 9.

In the IDIS model, a substrate-independent work function would correspond to charge transfer across the organic/metal interface with a screening factor $S = 0$, suggesting a very large $D(E_F)$; see equation (3). Hence, the IDIS model could be used to explain the TTF data, as well as the deviating points in the PFO and regio-regular P3HT studies mentioned previously. However, all of the substrates in the TTF study, as well as those in the PFO and P3HT studies, are of the 'dirty' variety, i.e. the surfaces are pacified by insulating monolayer(s). This should, according to the IDIS model, physically and electronically decouple the organic films from the continuum of the metallic electronic states of the substrates and hence yield a screening factor S close to 1 [21–23], not the 0 obtained from experiment! Clearly, a different description of the interface energetics is needed for these cases.

For conjugated polymer and molecule films, the integer charge transfer model does predict the observed independence of the substrate work function when $\Phi_{SUB} > E_{P+}/E_{BP++}$, i.e. when the substrate work function is larger than the formation energy of a positive polaron/bipolaron. This behaviour can be illustrated by a study on a number of ELPs spin-coated onto a variety of inorganic and organic metallic substrates that spanned over a wide range of work functions [14]. The following substrates were used in the study: aluminium with a native oxide layer ($\Phi_{SUB} = 3.8$–3.9 eV), silicon with a native oxide layer ($\Phi_{SUB} = 4.4$–4.5 eV), indium tin oxide as-received or ozone-treated ($\Phi_{SUB} = 4.7$–5.0 eV), ozone-treated gold ($\Phi = 5.2$–5.4 eV) and poly(3,4-ethylenedioxythiophene), PEDOT, with either poly(styrene sulfonic acid), PSS ($\Phi_{SUB} = 5.1$–5.4 eV), or poly(perfluoroethylene sulfonic acid), PFESA ($\Phi_{SUB} = 5.6$–6.1 eV), used as a counter ion. The choice of ELP materials reflects a large range of IPs: regio-regular poly(3-hexylthiophene) (P3HT), poly(dioctylfluorene-co-N-(4-butylphenyl)diphenylamine) (TFB), poly(9-(1′-decylundecylidene)fluorene) (P10AF), and PFO. The associated IP values are shown in table 1 [14]. UPS measurements were performed using monochromatized HeI, and the measurement sequence involved characterization of the bare substrates followed by spin-coating of the ELP material and subsequent characterization of the ELP-coated substrate. The substrate preparation and spin-coating was done under ambient (air) conditions.

Figure 10 [14] displays the dependence of $\Phi_{ELP/SUB}$ on the substrate work function, Φ_{SUB}, for the materials studied. Two distinct behaviours are clearly observed for all ELPs. For small

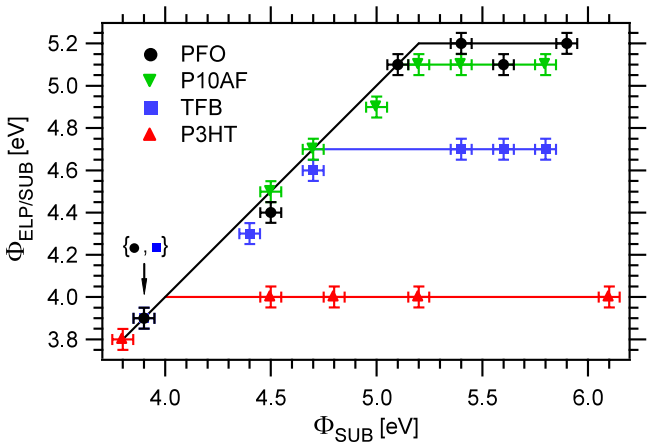

Figure 10. Dependence of work function of polymer coated substrate, $\Phi_{ELP/SUB}$, on the work function of bare substrate, Φ_{SUB}, for four materials studied, namely P3HT, TFB, P10AF and PFO.

Table 1. Estimates of essential parameters that characterize the energetics at the interface, as obtained by UPS measurements: ionization potential IP, polaronic energy and polaronic relaxation energy.

ELP	IP (±0.1 eV)	Polaronic energy (±0.1 eV)	Relaxation energy (±0.1 eV)
P3HT	4.5	4.0	0.5
TFB	5.4	4.7	0.7
P10AF	5.5	5.1	0.4
PFO	5.8	5.2	0.6

values of Φ_{SUB}, $\Phi_{ELP/SUB}$ scales linearly with a slope of unity with increasing Φ_{SUB}, i.e. no interfacial dipoles are formed and vacuum level alignment is obtained as discussed earlier. However, for values of Φ_{SUB} approaching and exceeding the polymer IPs, the $\Phi_{ELP/SUB}$ is independent of Φ_{SUB}, here mimicking the behaviour of the TTF study. The point where the behaviour goes from vacuum level alignment to a pinned, substrate-work-function-independent regime varies from ELP to ELP but seems roughly connected to the IP of the polymers. Note that the parameter S of the IDIS theory, if it were to be applied, would make a discrete jump from unity to zero where the vacuum level regime transforms into the Fermi level pinning regime. Hence, the same pacifying (mono)layer or insulating polymer layer that decouples some ELP films from the continuum of the metallic electronic states, yielding screening factors S close or equal to 1, allows for other ELPs so strong an interaction between the metallic continuum states and the valence states of the ELPs that a huge $D(E_F)$ is induced in the ELP band gap so that $S = 0$ is obtained, which is a highly unlikely scenario.

The pinning regime in figure 10 [14] displays shifts in the vacuum levels, indicating the formation of interfacial dipoles. Interestingly, the magnitudes of these energy shifts in the study are always such that the π-band edge of a particular ELP remains at a *constant* distance in energy from the Fermi level of the substrate and that the direction of the shifts indicates the formation of an interfacial dipole with the positive pole at the side of ELP. The results were interpreted using the integer charge transfer model [11–14]. As the Φ_{SUB} is increased up to the threshold value defined by the positive polaron/bipolaron formation energy for the ELP, i.e. the positive integer charge transfer state of a conjugated polymer, no charge is transferred across

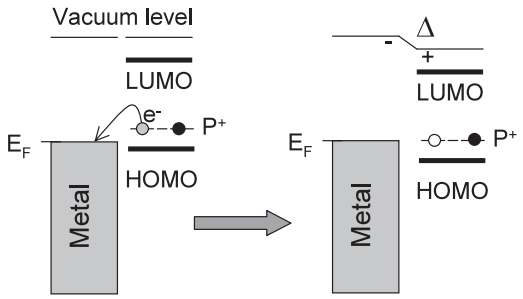

Figure 11. Schematic picture of the $\Phi_{SUB} > E_{P+}/E_{BP++}$ case where the polaron is the pinning state. When the energy needed to create a positive polaron is less than the energy gained by adding an electron to the metal substrate, charges (electrons) are transferred across the interface until equilibrium is reached, leaving the substrate Fermi level pinned to the half-filled polaron level (or band).

the interface. Above this threshold point however, charge is transferred at the interface from the ELP into the Fermi DOS of the substrate until equilibrium is reached; see figure 11. This implies that the resulting Fermi level will be pinned to the (polaronic) integer charge transfer states of the ELP at the interface. Note that the energy of the pinning level for each ELP in the study align identically at metallic or oxidized inorganic surfaces as well as at organic substrates (which, to a large extent, have an insulating layer at their surface). Consequently, the energy given by the pinning level likely carries information on the energy of polaronic levels in ELPs, albeit some modification thereof is expected, due to interface effects such as, for example, intra- and inter-chain ordering and screening from the substrate image charge. Table 1 [14] includes the values of the energies of the polaronic states inferred from the UPS data, along with IPs of the materials studied. By subtracting these energies from the value of respective IPs, estimates of the relaxation energies of the interface polaronic states, from 0.4 to 0.7 eV, are obtained, illustrating the important contribution of geometrical relaxation and substrate image charge screening to the interface polaronic formation energy, as the electronic relaxation contribution is expected to be ∼0.1 eV or less. This large spread in the relaxation values furthermore suggests that both polarons and bipolarons are possible pinning states, depending on which is the stable specie in the actual polymer in question (given the interface properties). These results showed that the interfaces of spin-coated polymers do not comply with the IDIS model, as the interfaces are clearly controlled by spontaneous charge transfer, or the lack thereof, into well-defined polaronic states of the ELPs, corresponding to either Fermi level pinning or vacuum level alignment regimes, respectively. In other words, the density of states in the polymer band gap peaks at the positive (negative) polaronic levels, but is negligible elsewhere in the gap.

Comparing these results with the PFO study [15], we see that the PFO-on-ozone-treated gold points that deviate from the vacuum level alignment regime (dashed line in figure 4) are located exactly at the polaronic-pinning energy of PFO, 5.2 eV. Similarly, we can interpret the TTF data [35] using the integer charge transfer model, placing the positive integer charge transfer level at ∼4.2 eV for the interface TTF molecules. Examples of pinning to negative integer charge transfer levels also exist in the literature, as illustrated in figure 12 [35]. Tetracyanoquinodimethane (TCNQ) molecules were deposited under UHV *in situ* conditions onto pacified metallic surfaces such as acetone and isopropanol washed (ozone-treated) gold, acetone and isopropanol washed indium tin oxide (ITO) and PEDOT-PSS. The work function of the samples, prior to and after TCNQ deposition, was measured by UPS. Below 4.8 eV of substrate work function, the TCNQ/substrate work function is substrate independent and pinned

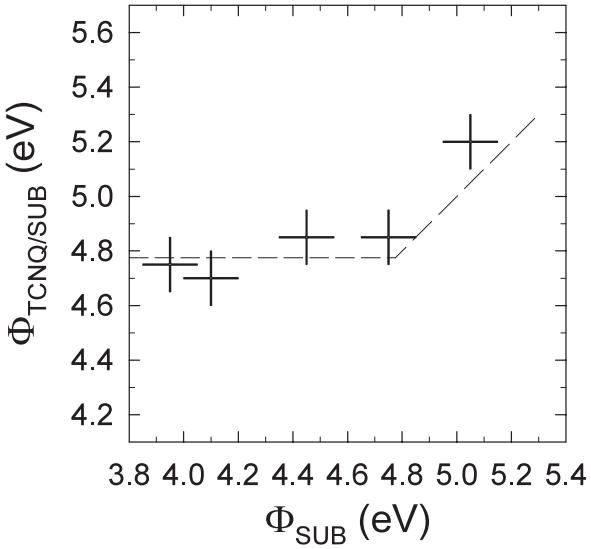

Figure 12. Dependence of work function of TTF *in situ* coated substrate, $\Phi_{TCNQ/SUB}$, on the work function of the bare substrate, Φ_{SUB}, as measured by UPS.

to ∼4.8 eV. For the data point above 4.8 eV of substrate work function however, the resulting TCNQ/substrate work function deviates from the pinning behaviour and instead follows a vacuum level alignment behaviour within the error bars of the measurement (±0.1 eV for both substrate and TCNQ/substrate work functions) [35]. In the pinning region, the interfacial dipole serves to upshift the original substrate work function, which means that the interfacial dipole created from charge transfer across the interface has its negative pole on the TCNQ side, i.e. the TCNQ molecules at the interface have accepted charge forming negative charge transfer states, likely singly occupied molecular orbitals derived from the LUMO of the neutral molecule. The study thus illustrate the cases of $\Phi_{SUB} < E_{ICT-}$ (negative integer charge transfer level pinning) and $E_{ICT-} < \Phi_{SUB} < EI_{CT+}$ (vacuum level alignment).

Though the experimental evidence is strong for applying the integer charge transfer model to describe energetics at weakly interacting organic/metal interfaces, much of the data could also be interpreted with the IDIS model as discussed so far in this paper. Indeed, by emphasizing the influence of a pacifying layer on the metallic substrates, be it hydrocarbon contamination or surface-segregated polyanions in conducting polymer blends, a screening factor of $S = 1$ (vacuum level alignment) could be justified for such interfaces. In contrast, the integer charge transfer model demands that spontaneous charge transfer can take place through such pacifying layers via tunnelling in order to justify the substrate-work-function-independent behaviour of some organic/metal interfaces. A key question then becomes whether such charge transfer is possible or not. Some of the data cited above suggest that indeed it can, but if the integer charge transfer model is correct and, for example, polaronic species are formed at the interface, they should show up in an UPS measurement, which is not the case in the data discussed. However, the integer charge transfer model assumes that, for the vast majority of cases, only the organic layer at the interface takes part in the charge transfer to/from the substrate. This in turn will prevent detection of integer charge transfer states such as polarons/bipolarons, since the films in the studies cited (typically >100 Å) were too thick compared to the probing depth of UPS (∼10 Å). The contradictory views on the pacifying layers present under ambient (air) conditions and in many conducting polymer blends have fortunately been resolved by a study of the existence and limits of spontaneous charge transfer between organic semiconductors and metals through insulating interfacial layers [38].

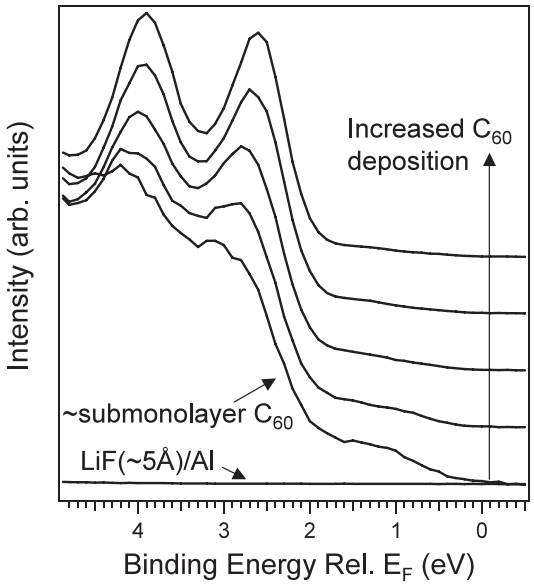

Figure 13. Evolution of the UPS measured frontier valence electronic structure of C_{60} films deposited *in situ* onto 5 Å LiF/Al substrates. The spectra are from C_{60} film thickness increasing from approximately submonolayer coverage to several monlayers, from bottom to top in the figure.

C_{60} and aluminium tris(8-hydroxyquinoline), Alq_3, molecules were deposited *in situ* under UHV conditions (base pressure $\sim 10^{-10}$ mbar) on two types of substrates: atomically clean aluminium (argon ion-sputtered prior to C_{60} and Alq_3 deposition) and a set of atomically clean aluminium substrates with LiF overlayers with thicknesses varying from 5–25 Å, also deposited *in situ* [38]. The evolution of the interface formation of these systems was probed using XPS and UPS. The evolution of the frontier valence electronic structure from a submonolayer up to a thick film of C_{60} on 5 Å LiF/Al is presented in figure 13 [38]. At low levels of coverage, an interfacial dipole is introduced and a new broad peak appears that extends between 1.5 and 0.5 eV versus the Fermi level. This feature does not appear in C_{60}/Al systems [38, 39]. As the coverage increases, the intensity of this feature decreases until the normal spectrum for bulk C_{60} is obtained, suggesting that the gap states are formed in the C_{60} molecules at the interface. The feature of the former HOMO level is slightly broader and a small shoulder is visible, similar to the case of C_{60}/Al, but weaker and less separated in energy ($\sim$0.4 eV peak split for C_{60}/Al [38, 39]). The significantly smaller perturbation of the HOMO level compared to the C_{60}/Al case is indicative of an absence of covalent bonding of C_{60} at the interface and is more in line with the results obtained from charge transfer (doping). Indeed, the gap state feature that appears upon (sub)monolayer coverage of C_{60} on top of LiF/Al is nearly identical, in both shape and binding energy position, to that of Rb_xC_{60} films, where $0.8 < x < 1$ [40], i.e. for C_{60} accepting $\sim$0.8–1 electron, assuming complete charge transfer from the alkali atom. From the XPS core level spectra of F(1s) and Li(1s) it is clear that the LiF molecule does not dissociate upon C_{60} deposition, which would be the only mechanism with which the LiF layer could provide charge to the C_{60} molecules. Hence, the electronic charge accepted by the C_{60} must be provided by the Al substrate. The frontier valence electronic structure obtained for C_{60} deposited on LiF/Al thus suggests that charge transfer (roughly $\sim$0.8–1 electron) occurs from the Al substrate through the LiF interfacial layer into the C_{60} molecules at the C_{60}/LiF interface (in turn producing an interfacial dipole). Such charge transfer (interface state and dipole) was found to occur for LiF interfacial layers less than 25 Å. For LiF $>$ 25 Å, no interface state was visible in the C_{60} valence spectrum and no change in interface dipole was detected upon C_{60} deposition.

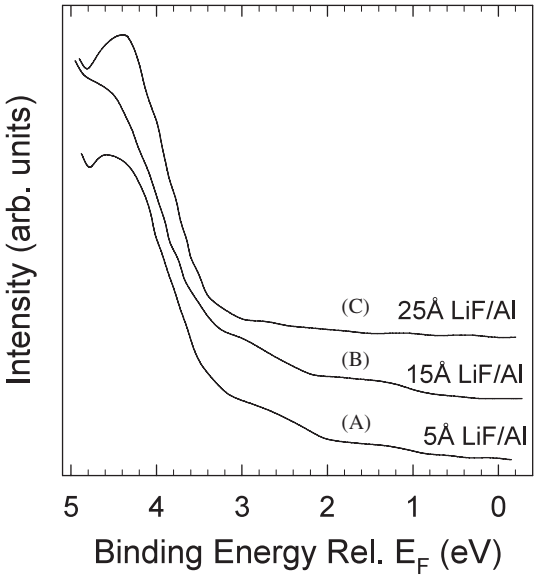

Figure 14. UPS spectra of submonolayer coverage Alq_3 films on (A) 5 Å LiF/Al, (B) 15 Å LiF/Al and (C) 25 Å LiF/Al, illustrating the disappearance of the interfacial states and hence spontaneous charge transfer for thick enough LiF layers.

The evolution of the frontier valence electronic structure from a submonolayer up to a thick film of Alq_3 on LiF/Al substrates showed similar behaviour [38]. Again, the XPS core level spectra of F(1s) and Li(1s) showed that the LiF molecule does not dissociate upon Alq_3 deposition (though this does occur upon the reverse order of deposition, Al/LiF/Alq_3 [41]). Here, for (sub)monolayer Alq_3 deposition onto LiF/Al substrates of LiF thickness of 5–15 Å, two gap states appear at lower binding energy than the peak derived from the original HOMO of Alq_3. The gap states were at a fixed binding energy position relative to the Fermi level, at 2.7 and 1.3 eV, respectively [38]. At 25 Å LiF thickness, the two gap states were not present; see figure 14 [38]. The single interface state that appears at ∼2.0 eV for Alq_3/Al interfaces [38, 42–44] did not appear for any of the Alq_3/LiF/Al systems, demonstrating that the Alq_3 molecules were not in direct contact with the aluminium substrate. The two new gap states must thus be the results of charge transfer between the Alq_3 monolayer and the Al substrate through the LiF sandwich layer, which takes place for an LiF thickness less than 25 Å. The evolution of the N(1s) core level was in agreement with charge transfer, though the core level shift was substantially smaller than the case of Li doping [41, 45]. The intensity of the gap states decreased upon increased coverage of Alq_3 until the standard spectrum for bulk Alq_3 was obtained, demonstrating that the charge transfer involves only the molecules at the interface, as is assumed for most cases in the integer charge transfer model. These studies show that spontaneous charge transfer between metal substrates and organic molecules can indeed occur through pacifying layers of substantial thickness, and that such charge transfer results in the formation of (integer charge transfer) gap states and interfacial dipoles, as per the integer charge transfer model.

The integer charge transfer model is further supported by device data and has its origin in device studies where transitions from substrate-dependent injection barriers to substrate-independent injection barriers were demonstrated. Studies on metal/MEH-PPV/metal devices using electroabsorption measurements of built-in electric fields and internal photoemission measurements of Schottky barriers yielded the ‘Mark of Zorro’ dependence on the substrate work function that is expected from the integer charge transfer model [13]. In those studies, bipolarons were found to be the pinning state of MEH-PPV [13].

4. Summary and discussion

We have described the competing models for describing the energetics at weakly interacting organic/metal interfaces, i.e. organic-on-metal and metal-on-organic interfaces where no bond formation occurs but charge transfer across the interface can take place. The models discussed are not generally applicable to metal/organic interfaces involving covalent bonding or doping, and such interfaces usually have to be studied experimentally on a system-by-system basis. We have argued in favour of the so-called integer charge transfer model for the weakly interacting interfaces that will typically be formed when surfaces and/or film depositions have been prepared in high-to-low vacuum and ambient atmosphere/glovebox conditions. The integer charge transfer model states that, for metal electrode (substrate) work functions that are smaller than the positive integer charge transfer level and larger than the negative integer charge transfer level of the organic film, no spontaneous charge transfer across the interface occurs and vacuum level alignment is observed. For substrate (electrode) work functions that are larger than the positive integer charge transfer level (or smaller than the negative integer charge transfer level), spontaneous charge transfer across the interface occurs and the Fermi level is pinned to the positive (negative) integer charge transfer level. Hence, the injection barrier at a vacuum level aligned interface will depend linearly on the difference between the metal electrode (substrate) work function and the formation energy of the integer charge transfer level. For the particular case of large conjugated molecules and polymers, where the integer charge transfer states are polaronic in nature, the injection barrier at a pinned interface may be ohmic if the Fermi level is pinned to a polaron level and small but non-negligible if pinned to a bipolaron level. Hence, to predict the injection barriers in such a device, we need to know the metal electrode (substrate) work functions and the polaronic formation energies of the organic material.

Note that it is the work function of the *pacified* metal electrode (substrate) that is the relevant parameter, not the work function of the atomically clean metal surface. The so-called push-back effect, i.e. a decrease in the metal work function caused by a shortening of the electron density tail at the metal surface due to physisorbed species, is often significant and always occurs both for organic-on-metal and metal-on-organic interfaces, even when prepared under UHV conditions. Determining the integer charge transfer level energies is complicated as well, in particular for the case of conjugated large molecules and polymers. Here, the relevant parameter is the polaronic formation energy for the organic molecules/polymers at the *interface*, not in the bulk, and those energies can be different for a variety of reasons. Perhaps the main influence comes from ordering effects of the organic film at the interface. For polymers, improved order at the interface compared to the bulk may lead to extended (less coiled) chains. Extended chains imply longer conjugation lengths, which in turn will increase (decrease) the positive (negative) polaronic formation energies, as the polaronic species can extend over a larger segment of the polymer chain. For highly ordered polymer and molecular films at the interface, interchain and intermolecular polaronic states may be formed that will further increase (decrease) the positive (negative) formation energies. The polaronic formation energy, and hence the pinning energy, also may be affected by screening from the substrate (image potential) and by the surrounding dielectric medium. This effect likely is an important factor contributing to the large relaxation energies obtained for the polymer systems discussed, and further note that the image charge screening effect will also be present in systems where the integer charge transfer states are not polaronic but merely derived from the HOMO and LUMO of the neutral molecules. Ordering of the organic molecules at the interface can also play a role if the molecules have an intrinsic dipole, which of course would affect the energetics of the interface.

The effects that are discussed are not of academic interest only but play an important role in device design. For instance, the integer charge transfer model might, at first glance, suggest

that it may not be worthwhile to pursue the development of extremely high (or low) work function materials for anode (and cathode) electrodes, as the effective work function of the metal electrodes needs just to fulfill the $\Phi_{SUB} > E_{ICT+}$ or $\Phi_{SUB} < E_{ICT-}$ requirements for (near) ohmic contact. Care should be taken when pursuing this argument however, as some conducting polymer blends used as hole-injecting layers are known to undergo a decrease in work function over time, and hence what may be a pinned interface upon post-production testing will be a vacuum level aligned interface with a substantial injection barrier after some time in storage or use, if the initial anode work function was too closely matched to E_{ICT+}. Ordering effects may cause the same problems. An initially disordered organic film at the anode contact may, over time and driving-induced heat, become more ordered, increasing the polaronic formation energy and thus changing the contact from ohmic to one with a barrier (vacuum level alignment). The reverse scenario is also possible; a well-ordered interface designed to have a fixed barrier at the hole-injecting contact may find the barrier decreased or even pushed into an ohmic regime by heat-induced disorder of the organic film. Yet another scenario is where order dramatically decreases the band gap of the polymer films and hence decreases the positive polaronic formation energy. Corresponding effects at electron-injecting contacts are equally possible, of course. The ordering effects are less likely to play a role for electroluminescent polymers, as most of them are designed to form disordered, amorphous layers and films. For electroluminescent molecules, and molecules/polymers synthesized for use in transistors, order/disorder effects on polaronic formation energies and hence on device design and device performance over time warrant attention, as such materials are more likely to order well. In particular, different ink formulations may lead to different orderering at the interface for ink-jet printed films. Note that the key factor is film order at the *interface*, as it is the molecules and polymers at the interface that participate in the charge transfer with the substrate.

Finally, we stress that the models for weakly interacting interfaces should not be applied where there is chemisorption. Covalent bonding between organic molecules and metals typically leads to the introduction of sp^3 defects in the π-conjugation of the organic materials or chemical doping that significantly changes their electronic structure and properties [37, 46–51]. Such strongly interacting interfaces, typically formed when reactive metal atoms are deposited on organic films or when organic molecules are deposited onto atomically clean metal surfaces under UHV conditions, should be studied on a case-per-case basis, as the exact interfacial chemistry and its effects are hard to predict. For the latter case, i.e. molecules deposited under UHV conditions on clean metal surfaces, the IDIS model has shown good applicability, as the chemical and physical realities of such interfaces are in line with the basic assumptions of the model.

References

[1] Fahlman M and Salaneck W R 2002 *Surf. Sci.* **500** 904
[2] Haskal E I, Büchel M, Duineveld P C, Sempel A and van de Weijer P 2002 *MRS Bull.* **27** 864
[3] Dimitrakopoulos C D and Malenfant P R L 2002 *Adv. Mater.* **14** 99
[4] Brabec C J, Sariciftci N S and Hummelen J C 2001 *Adv. Funct. Mater.* **11** 15
[5] Ma W, Yang C, Gong X, Lee K and Heeger A J 2005 *Adv. Funct. Mater.* **15** 1617
[6] Chen J and Reed M A 2002 *Chem. Phys.* **281** 127
[7] Chen J, Reed M A, Rawlett A M and Tour J M 1999 *Science* **286** 1550
[8] Reed M A, Zhou C, Muller C J, Burgin T P and Tour J M 1997 *Science* **278** 252
[9] Vazquez H, Flores F, Oszwaldowski R, Ortega J, Perez R and Kahn A 2004 *Appl. Surf. Sci.* **234** 107
[10] Vázquez H, Gao W, Flores F and Kahn A 2005 *Phys. Rev.* B **71** 041306(R)
[11] Davids P S, Saxena A and Smith D L 1995 *J. Appl. Phys.* **78** 4244
[12] Davids P S, Saxena A and Smith D L 1996 *Phys. Rev.* B **53** 4823
[13] Campbell I H, Hagler T W, Smith D L and Ferraris J P 1996 *Phys. Rev. Lett.* **76** 1900

[14] Tengstedt C, Osikowicz W, Salaneck W R, Parker I D, Hsu C-H and Fahlman M 2006 *Appl. Phys. Lett.* **88** 053502
[15] Greczynski G, Fahlman M and Salaneck W R 2000 *Chem. Phys. Lett.* **321** 379
[16] Siegbahn K, Nordling C, Fahlman A, Nordgerg R, Hamrin K, Hedman J, Johansson G, Bergmark T, Karlsson S E, Lindgren I and Lindgren B 1967 *ESCA-Atomic, Molecular and Solid State Structure Studied by Means of Electron Spectroscopy* (Uppsala: Almqvist and Wiksells)
[17] Turner D W, Baker C, Baker A D and Brundle C R 1970 *Molecular Photoelectron Spectroscopy* (London: Interscience)
[18] Beamson G and Briggs D 1992 *High Resolution XPS of Organic Polymers* (New York: Wiley)
[19] Fadley C S 1978 *Electron Spectroscopy: Theory, Techniques and Applications* ed C R Brundle and A D Baker (London: Academic) p 1
[20] Osikowicz W, de Jong M P, Braun S, Tengstedt C, Fahlman M and Salaneck W R 2006 *Appl. Phys. Lett.* **88** 193504
[21] Hwang J, Amy F and Kahn A 2006 *Org. Electron.* **110** 14363
[22] Wan A, Hwang J, Amy F and Kahn A 2005 *Org. Electron.* **6** 47
[23] Vazquez H, Oszwaldowski R, Pou P, Ortega J, Perez P, Flores F and Kahn A 2004 *Europhys. Lett.* **65** 802
[24] Greczynski G, Kugler T, Keil M, Osikowicz W, Fahlman M and Salaneck W R 2001 *J. Electron. Spectrosc. Relat. Phenom.* **121** 1
[25] Jönsson S K M, Birgerson J, Crispin X, Greczynski G, Osikowicz W, v d Gon A W D, Salaneck W R and Fahlman M 2003 *Synth. Met.* **139** 1
[26] Tengstedt C, Crispin A, Hsu C, Skulason H, Parker I D, Salaneck W R and Fahlman M 2005 *Org. Electron.* **6** 21
[27] Lang N D 1981 *Phys. Rev. Lett.* **46** 842
[28] Bagus P S, Staemmler V and Wöll C 2002 *Phys. Rev. Lett.* **89** 096104
[29] Crispin X, Geskin V M, Crispin A, Cornil J, Lazzaroni R, Salaneck W R and Brédas J L 2002 *J. Am. Chem. Soc.* **124** 8131
[30] Crispin X, Lazzaroni R, Crispin A, Geskin V M, Brédas J L and Salaneck W R 2001 *J. Electron. Spectrosc. Relat. Phenom.* **121** 57
[31] Lang N D and Kohn W 1973 *Phys. Rev.* B **7** 3541
[32] Lang N D and Kohn W 1970 *Phys. Rev.* B **3** 1215
[33] Chen Y C, Cunningham J E and Flynn C P 1984 *Phys. Rev.* B **30** 7317
[34] Kugler T, Salaneck W R, Rost H and Holmes A B 1999 *Chem. Phys. Lett.* **310** 391
[35] Murdey R J and Salaneck W R 2005 *Japan. J. Appl. Phys.* **44** 3751
[36] Ishii H, Sugiyama K, Ito E and Seki K 1999 *Adv. Mater.* **11** 605
[37] Salaneck W R, Seki K, Kahn A and Pireaux J J (ed) 2002 *Conjugated Polymer and Molecular Interfaces: Science and Technology for Photonic and Optoelectronic Application* (New York: Dekker)
[38] Jönsson S K M, Salaneck W R and Fahlman M 2005 *J. Appl. Phys.* **98** 14901
[39] Maxwell A J, Brühwiler P A, Arvanitis D, Hasselström J, Johansson M K-J and Mårtensson N 1998 *Phys. Rev.* B **57** 7312
[40] Chase S J, Mitch M G, Lannin J S and Olson C G 1998 *Phys. Rev.* B **58** 15491
[41] Mason M G, Tang C W, Hung L-S, Raychaudhuri P, Madathil J, Giesen D J, Yan L, Le Q T, Gao Y, Lee S-T, Liao L S, Cheng L F, Salaneck W R, d Santos D A and Bredas J L 2001 *J. Appl. Phys.* **89** 2756
[42] Yoshimura D, Yokoyama T, Ito E, Ishii H, Ouchi Y, Hasegawa S and Seki K 1999 *Synth. Met.* **102** 1145
[43] Yokoyama T, Yoshimura D, Ito E, Ishii H, Ouchi Y and Seki K 2003 *Japan. J. Appl. Phys.* 1 **42** 3666
[44] Ishii H, Yoshimura D, Sugiyama K, Hamatani Y, Kawamoto I, Miyazaki T, Ouchi Y and Seki K 1997 *Synth. Met.* **85** 1389
[45] Johansson N, Osada T, Stafström S, Salaneck W R, Parente V, d Santos D A, Crispin X and Brédas J L 1999 *J. Chem. Phys.* **111** 2157
[46] Dannetun P, Fahlman M, Fauquet C, Kaerijama K, Sonoda Y, Lazzaroni R, Brédas J L and Salaneck W R 1994 *Organic Materials for Electronics: Conjugated Polymer Interfaces with Metals and Semiconductors* ed J L Brédas, W R Salaneck and G Wegner (Amsterdam: North-Holland) p 113
[47] Dannetum P, Boman M, Stafström S, Salaneck W R, Lazzaroni R, Fredriksson C, Brédas J L, Zamboni R and Taliani C 1993 *J. Chem. Phys.* **99** 664
[48] Fahlman M, Beljonne D, Lögdlund M, Burn P L, Holmes A B, Friend R H, Brédas J L and Salaneck W R 1993 *Chem. Phys. Lett.* **214** 327
[49] Fahlman M, Moratti S, Holmes A B, Salaneck W R and Brédas J L 1997 *Chem. Eur. J.* **3** 286
[50] Lögdlund M and Brédas J L 1994 *J. Chem. Phys.* **101** 4357
[51] Jönsson S K M, de Jong M P, Groenendaal L, Salaneck W R and Fahlman M 2003 *J. Phys. Chem.* B **107** 10793